

PREPARED FOR SUBMISSION TO JCAP

Primordial Tensor Non-Gaussianity from Massive Gravity

Tomohiro Fujita,^{a,b} Shuntaro Mizuno^c and Shinji Mukohyama^{d,e}

^aDepartment of Physics, Kyoto University, Kyoto, 606-8502, Japan

^bDépartement de Physique Théorique and Center for Astroparticle Physics,
Université de Genève, Quai E. Ansermet 24, CH-1211 Genève 4, Switzerland

^cDepartment of Liberal Arts and Engineering Sciences,
National Institute of Technology, Hachinohe college, Aomori 039-1192, Japan

^dCenter for Gravitational Physics, Yukawa Institute for Theoretical Physics,
Kyoto University, Kyoto 606-8502, Japan

^eKavli Institute for the Physics and Mathematics of the Universe (WPI),
The University of Tokyo Institutes for Advanced Study,
The University of Tokyo, Kashiwa, Chiba 277-8583, Japan

Abstract. We calculate tensor bispectrum in a theory of massive tensor gravitons which predicts blue-tilted and largely amplified primordial gravitational waves. We find that a new 3-point interaction can produce a larger tensor bispectrum than the conventional one from general relativity. The bispectrum peaks at the squeezed configuration and its slope towards the squeezed limit is determined by the graviton mass. This squeezed tensor bispectrum may be observed as the quadrupolar modulation of the tensor power spectrum by interferometers.

Contents

| | | |
|----------|---|-----------|
| 1 | Introduction | 1 |
| 2 | Dynamics of Massive Graviton | 3 |
| 3 | Tensor Bispectrum | 5 |
| 3.1 | Evaluating time integral during inflation | 7 |
| 3.2 | Evolution after inflation | 8 |
| 3.3 | Tensor bispectrum today | 9 |
| 4 | Quadrupolar modulation of tensor power spectrum | 11 |
| 5 | Conclusions and Discussions | 14 |
| A | Graviton mass and coupling constant in MTMG Theory | 15 |
| B | Real Part versus Imaginary Part | 16 |

1 Introduction

Cosmic inflation is widely believed to be the most plausible explanation for the origin of primordial perturbations in our Universe, while it is still nontrivial to embed inflation into more fundamental theories (see [1], for a review). Inflation predicts the existence of primordial gravitational waves (GWs), whose power spectrum amplitude depends on the value of the Hubble expansion rate during inflation (see [2], for a review). In order to detect or put constraints on the primordial GWs, there are future/ongoing experiments of Cosmic Microwave Background (CMB) B-mode polarization like Lite BIRD [3] as well as interferometers such as LISA [4], Advanced-LIGO (A-LIGO) [5] and DECIGO [6, 7]. In most models of inflation, the power spectrum of primordial GWs is almost scale invariant, with a slightly red tilt, where the most promising way to detect the primordial GWs is through CMB B-mode polarization. Nevertheless, it should be stressed that even if inflation occurred, there are scenarios where the amplitude of primordial GWs can be amplified at scales much smaller than CMB's (see for reviews, [8, 9]). These scenarios are observationally interesting, since they open up the possibility that the primordial GWs can be detected by interferometer experiments, even if their signal is not observed at the CMB scale.¹

Among the various scenarios showing interesting features for the primordial GWs at small scales, massive gravity (see [11], for a review) attracts conspicuous attention and has been applied to the study on the primordial GWs [12–15]. In this context, recently we have proposed a new scenario predicting blue-tilted and largely amplified primordial GWs [16]. This prediction is based on the two assumptions, where the first one is that the mass of tensor graviton is comparable to the Hubble expansion rate during the inflation and the second one is that the mass diminishes to a small value at a certain time during radiation dominated era. Owing to the first assumption, the power spectrum of primordial GWs is

¹However, recently a new method was proposed to constrain the amplitude of the primordial GWs from the CMB data at Mpc scale, see [10].

blue at the end of inflation. From the second one, after inflation until the mass diminishes to a small value, gravitons are diluted as non-relativistic matter and hence their amplitude can be substantially amplified compared to the conventional massless gravitons which decay as radiation. In conventional massive gravity theories including the one proposed by de Rham-Gabadadze-Tolley (dRGT) [17, 18], it is well known that the tensor graviton mass that is positive and comparable to the Hubble expansion rate is prohibited around de Sitter background by the so-called Higuchi bound [19]. Contrary to this, however, there are viable theories in which the graviton mass in such region does not introduce instabilities, like the minimal theory of massive gravity (MTMG) [20, 21]. In MTMG, there are only two physical degrees of freedom propagating as in general relativity in the gravity sector and the would be ghost mode is removed from the construction, where the assumption of the Lorentz-invariance is relaxed (see [22–27] for works considering interesting phenomenology based on Lorentz-violating massive gravity).

The scenario of [16] has similarity with the one of [28] based on a generalization of solid inflation [29, 30] dubbed supersolid inflation [31] (see [32–34] for related works). Supersolid inflation is a scenario that simultaneously breaks time reparameterization and spatial diffeomorphisms during inflation based on the Effective Field Theory (EFT) of inflation [35]. Such a symmetry breaking pattern is accompanied by the appearance of the tensor graviton mass that can be comparable to the Hubble expansion rate during inflation without introducing ghost instability. Therefore, the fact that the graviton mass comparable to the Hubble expansion rate during inflation makes the primordial GWs blue-tilted holds in both scenarios. The mechanism to enhance the primordial GWs so that it is detectable by interferometers, however, is different. Since supersolid inflation is based on EFT of inflation described by four scalar fields having time- and space-dependent *vevs* which break reparameterization symmetries of the background, at the end of inflation, these fields are regarded to arrange themselves so that the space-reparameterization symmetry is recovered. Therefore, in the scenario of [28], the mass of tensor graviton becomes zero at the end of inflation, where the enhancement mechanism in the scenario of [16] is not applicable.²

Given the situation that there are several scenarios that predict primordial GWs detectable at interferometer scales, it is important to think about how to distinguish them. In this respect, the statistical property of primordial GWs is a very helpful tool, as in the case of primordial curvature perturbations. For example, the primordial GWs from vacuum fluctuations of the metric are almost Gaussian [36, 37]. Furthermore, stochastic gravitational wave backgrounds due to a combination of a large number of uncorrelated astrophysical sources is Gaussian to a high degree, due to the central limit theorem. Therefore, in this paper, we calculate the bispectrum of primordial GWs, which is the lowest order statistics providing information on non-Gaussianity of tensor fluctuations, depending on not only the amplitude, but also the shape of the triangle composed of the three momentum vectors in the scenario of [16] (for other works discussing tensor non-Gaussianity, see [38–48]).

It seems that the simplest way to detect the primordial tensor bispectrum is the direct measurement of the bispectrum at interferometer scales [49]. However, it was shown that the bispectrum cannot be probed directly [50, 51]. This is caused by the fact that the tensor bispectrum at small scales is suppressed due to Shapiro time-delay effects associated with the propagation of tensor modes at sub-horizon scales in the presence of matter. On the other hand, for supersolid inflation, another method to prove the tensor bispectrum based on

²In the scenario of [28], it is possible to obtain the primordial GWs detectable by interferometers by considering small speed of sound for the tensor perturbations.

the quadrupolar modulation of the tensor power spectrum induced by the tensor bispectrum was proposed [28].³ As mentioned above, since there is similarity between Lorentz-violating massive gravity and supersolid inflation, it is expected that the quadrupolar modulation of the tensor power spectrum is also induced in the Lorentz-violating massive gravity. Therefore, we calculate the quadrupolar modulation of the tensor power spectrum induced by the tensor bispectrum and briefly discuss the detectability.⁴

The rest of this paper is organized as follows. In section 2, we briefly summarize the result on the tensor power spectrum in the scenario of [16]. Then, in section 3, we calculate the tensor bispectrum in the same scenario today based on the in-in formalism. In section 4, we calculate the quadrupolar modulation of the tensor power spectrum sourced by the tensor bispectrum and consider the detectability. Section 5 is devoted to conclusions and discussions.

2 Dynamics of Massive Graviton

Here, we briefly explain our setup which was developed in Ref. [16]. Our quadratic action for the tensor graviton $h_{ij}(\tau, \mathbf{x})$ is given by

$$S_h^{(2)} = \frac{M_{\text{Pl}}^2}{8} \int d\tau d^3x a^2 [h'_{ij} h'_{ij} - \partial_l h_{ij} \partial_l h_{ij} - a^2 \mu^2 h_{ij} h_{ij}] , \quad (2.1)$$

where M_{Pl} is the reduced Planck mass, $a(\tau)$ is the scale factor, $\mu(\tau)$ is the mass of the tensor graviton, τ is the conformal time and a prime denotes its derivative, i.e. $X' \equiv \partial_\tau X$. The tensor gravitons can be decomposed and quantized as

$$h_{ij}(\tau, \mathbf{x}) = \frac{2}{a M_{\text{Pl}}} \sum_{\lambda=+,-} \int \frac{d^3k}{(2\pi)^3} e^{i\mathbf{k}\cdot\mathbf{x}} e_{ij}^\lambda(\hat{\mathbf{k}}) \left[v_k^\lambda(\tau) \hat{a}_{\mathbf{k}}^\lambda + \text{h.c.} \right] , \quad (2.2)$$

where $e_{ij}^\lambda(\hat{\mathbf{k}})$ is the polarization tensor and $\hat{a}_{\mathbf{k}}/\hat{a}_{\mathbf{k}}^\dagger$ are creation/annihilation operators satisfying the commutation relation, $[\hat{a}_{\mathbf{k}}^\lambda, \hat{a}_{\mathbf{p}}^{\dagger\sigma}] = (2\pi)^3 \delta^{\lambda\sigma} \delta(\mathbf{k} - \mathbf{p})$.⁵ Henceforth, we often suppress the polarization label λ when it is not relevant.

To obtain the evolution of the mode function v_k , we need to specify $a(\tau), \mu(\tau)$ and the initial condition for $v_k(\tau)$. For simplicity, we assume the de Sitter expansion $a \propto \tau^{-1}$ during inflation as well as instantaneous reheating followed by the radiation dominated era $a \propto \tau$, which gives

$$a(\tau) = \begin{cases} -1/(H_{\text{inf}}\tau) & (\tau < -\tau_r) \\ a_r \tau / \tau_r & (\tau > \tau_r) \end{cases} . \quad (2.3)$$

Here H_{inf} is the Hubble expansion rate during inflation and a_r is the scale factor at the reheating time $\tau_r = (a_r H_{\text{inf}})^{-1}$. Note that in this treatment the conformal time τ jumps

³The idea that the squeezed tensor bispectrum induces the quadrupolar modulation of the power spectrum of curvature perturbation was proposed earlier and has been investigated actively in the name of ‘tensor fossils’ [52–55].

⁴For the discussion on the detection of primordial GWs with pulsar timing arrays like SKA [56], see [57].

⁵The polarization tensor $e_{ij}^\lambda(\hat{\mathbf{k}})$ generally satisfies the transverse-traceless condition $k_i e_{ij}^\lambda(\hat{\mathbf{k}}) = e_{ii}^\lambda(\hat{\mathbf{k}}) = 0$. Since we employ the circular polarization tensor, we also have the normalization conditions $e_{ij}^{\lambda*}(\hat{\mathbf{k}}) e_{ij}^{\lambda'}(\hat{\mathbf{k}}) = \delta_{\lambda\lambda'}$ and the following properties $e_{ij}^{\lambda*}(\hat{\mathbf{k}}) = e_{ij}^{-\lambda}(\hat{\mathbf{k}}) = e_{ij}^\lambda(-\hat{\mathbf{k}})$ for $\lambda = \pm$.

from $-1/(aH_{\text{inf}})$ into $1/(aH_{\text{inf}})$ at reheating for a and $da/d\tau$ to be continuous. We further assume a simple step-function behavior of the graviton mass,

$$\mu(\tau) = \begin{cases} m & (\tau < \tau_m) \\ 0 & (\tau > \tau_m) \end{cases}, \quad (2.4)$$

where τ_m is a certain time during radiation dominated era. Finally, we set the initial condition for the mode function to be that for the Bunch-Davies vacuum during inflation,

$$\lim_{k\tau \rightarrow -\infty} v_k(\tau) = \frac{1}{\sqrt{2k}} e^{-ik\tau}. \quad (2.5)$$

Solving the equation of motion (EoM) based on the above setup, one can show that the mode function $v_k(\tau)$ during inflation is given by

$$v_k(\tau < \tau_r) = \frac{\sqrt{-\pi\tau}}{2} H_\nu^{(1)}(-k\tau), \quad \nu \equiv \sqrt{\frac{9}{4} - \frac{m^2}{H_{\text{inf}}^2}}. \quad (2.6)$$

where $H_\nu^{(1)}$ is the Hankel function of the first kind of order ν . To discuss the mode function during inflation in more detail, it is useful to introduce a new dimensionless time variable $x \equiv -k\tau$. Well after the horizon exit, $x \ll 1$, the mode function has the asymptotic form

$$\lim_{x \rightarrow 0} v_k(x) = \sqrt{\frac{\pi}{2k}} \left[\frac{1}{\Gamma(1+\nu)} \left(\frac{x}{2}\right)^{\frac{1}{2}+\nu} - i \frac{\Gamma(\nu)}{\pi} \left(\frac{x}{2}\right)^{\frac{1}{2}-\nu} \right], \quad (\tau < \tau_r), \quad (2.7)$$

where $\Gamma(\nu)$ is the gamma function. Although the second term is always dominant in the magnitude, the first term which carries the real part of v_k also plays an important role in the calculation of the tensor bispectrum, as we will see in the next section.

The ratio of the mode functions between the current massive case ($v_k^{\text{massive}}(\tau)$) and the usual massless case ($v_k^{\text{massless}}(\tau)$) is evaluated at the end of inflation as

$$\Upsilon_k(\tau) \equiv \left| \frac{v_k^{\text{massive}}(\tau)}{v_k^{\text{massless}}(\tau)} \right| \implies \Upsilon_k(\tau_r) \simeq \frac{\Gamma(\nu)}{\Gamma(3/2)} \left| \frac{k\tau_r}{2} \right|^{\frac{3}{2}-\nu}. \quad (2.8)$$

Since $|k\tau_r| \ll 1$ and $\nu < 3/2$ for the massive graviton on super-horizon scales, the mode function is suppressed compared to the conventional massless case. On the other hand, after inflation ends and the Hubble expansion rate H decreases, the super-horizon graviton modes behave as non-relativistic matter with $m > H > k/a$. Then the mode function is relatively amplified, $\Upsilon_k \propto a^{1/2}$, compared to the massless graviton modes which behave as radiation. This amplification continues until the graviton mass vanishes at $\tau = \tau_m$. The ratio of the mode functions is then given by [16]

$$\Upsilon_k(\tau \gg \tau_m) = \gamma_k \sqrt{\frac{\tau_m}{\tau_r}} \frac{\Gamma(\nu)}{\Gamma(3/2)} \left| \frac{k\tau_r}{2} \right|^{\frac{3}{2}-\nu}, \quad (2.9)$$

where γ_k has a rather lengthy expression obtained by solving the junction conditions, but it is $\mathcal{O}(1)$ for $m/H_{\text{inf}} \sim 1$. As a result, the dimensionless power spectrum of the tensor modes is written as [16]

$$\mathcal{P}_h(k, \tau \gg \tau_m) = \tilde{\gamma}_k^2 |k\tau_r|^{3-2\nu} \frac{\tau_m}{\tau_r} \mathcal{P}_h^{\text{massless}}(k, \tau), \quad (2.10)$$

with $\tilde{\gamma}_k \equiv \gamma_k \times 2^{\nu-3/2} \Gamma(\nu)/\Gamma(3/2)$. Here, $\mathcal{P}_h^{\text{massless}}$ denotes the usual power spectrum of the massless tensor modes from inflation,

$$\mathcal{P}_h^{\text{massless}}(k, \tau) = \mathcal{T}_k^2(\tau) \frac{2H_{\text{inf}}^2}{\pi^2 M_{\text{Pl}}^2}, \quad (2.11)$$

with the transfer function of the massless tensor modes,

$$\mathcal{T}_k(\tau) \equiv \frac{h_k^{\text{massless}}(\tau)}{h_k^{\text{massless}}(\tau_r)} = \frac{a(\tau_r) v_k^{\text{massless}}(\tau)}{a(\tau) v_k^{\text{massless}}(\tau_r)}. \quad (2.12)$$

If gravitons keep the mass for a while after inflation $\tau_m \gg \tau_r$, it overcomes the dumping factor in Eq. (2.8) and the gravitational waves can be substantially amplified for relevant modes with $|k\tau_r|^{3-2\nu} \tau_m/\tau_r \gg 1$. The tensor tilt is

$$n_T \equiv \frac{d \ln \mathcal{P}_h(\tau_r)}{d \ln k} = 3 - 2\nu, \quad (2.13)$$

where the $\mathcal{O}(\epsilon_H)$ slow-roll correction is ignored under the assumption $m/H_{\text{inf}} = \mathcal{O}(1)$. Notice that the tilt of the power spectrum is blue, $n_T > 0$, because the mode function decays on super-horizon scales during inflation.

3 Tensor Bispectrum

In this section, we calculate the tensor bispectrum. We consider the following interaction Hamiltonian at the third order for the tensor perturbation:

$$H_{\text{int}} = H_{\text{int}}^{(\text{GR})} + H_{\text{int}}^{(\text{mass})}, \quad (3.1)$$

with

$$H_{\text{int}}^{(\text{GR})} = -\frac{M_{\text{Pl}}^2}{4} a^2 \int d^3x h_{ij} h_{kl} \left(\partial_j \partial_l h_{ik} - \partial_i \partial_j \frac{1}{2} h_{kl} \right), \quad (3.2)$$

$$H_{\text{int}}^{(\text{mass})} = -g \frac{M_{\text{Pl}}^2}{4} a^4 \int d^3x h_{ij} h_{jk} h_{ki}, \quad (3.3)$$

where the coefficient $g(\tau)$ depends on time. $H_{\text{int}}^{(\text{GR})}$ is found even in general relativity (GR) around de Sitter space. On the other hand, $H_{\text{int}}^{(\text{mass})}$ is absent in GR and it arises from the same argument as the graviton mass term as discussed in appendix A. We assume g is also constant during inflation in the same way as the graviton mass μ (see eq. (2.4)). It is worth mentioning that $H_{\text{int}}^{(\text{mass})}$ also appears in supersolid inflation [28, 34], which suggests that the appearance of this interaction is a generic feature of the breaking of the space reparameterization symmetry.

The three-point function for the tensor mode h_{ij} can be calculated based on the in-in formalism [36, 58],

$$\langle h_{i_1 j_1}(\tau, \mathbf{k}_1) h_{i_2 j_2}(\tau, \mathbf{k}_2) h_{i_3 j_3}(\tau, \mathbf{k}_3) \rangle = i \int_{-\infty}^{\tau} d\eta \langle [H_{\text{int}}(\eta), h_{i_1 j_1}(\tau, \mathbf{k}_1) h_{i_2 j_2}(\tau, \mathbf{k}_2) h_{i_3 j_3}(\tau, \mathbf{k}_3)] \rangle. \quad (3.4)$$

From this three-point function, we define un-contracted bispectrum for later convenience as

$$\langle h_{i_1 j_1}(\tau, \mathbf{k}_1) h_{i_2 j_2}(\tau, \mathbf{k}_2) h_{i_3 j_3}(\tau, \mathbf{k}_3) \rangle \equiv (2\pi)^3 \delta(\mathbf{k}_1 + \mathbf{k}_2 + \mathbf{k}_3) B_{i_1 j_1 i_2 j_2 i_3 j_3}(k_1, k_2, k_3), \quad (3.5)$$

where $k_i \equiv |\mathbf{k}_i|$. Taking the following sum over the indices, one can compute the tensor bispectrum from it,

$$B_h(k_1, k_2, k_3) = \delta_{j_1 i_2} \delta_{j_2 i_3} \delta_{j_3 i_1} B_{i_1 j_1 i_2 j_2 i_3 j_3}(k_1, k_2, k_3). \quad (3.6)$$

The un-contracted bispectrum $B_{i_1 j_1 i_2 j_2 i_3 j_3}$ can be split into two parts which are contributed by $H_{\text{int}}^{(\text{GR})}$ and $H_{\text{int}}^{(\text{mass})}$, respectively, as

$$B_{i_1 j_1 i_2 j_2 i_3 j_3} = B_{i_1 j_1 i_2 j_2 i_3 j_3}^{(\text{GR})} + B_{i_1 j_1 i_2 j_2 i_3 j_3}^{(\text{mass})}. \quad (3.7)$$

Plugging eqs. (3.2) and (3.3) into (3.4), we obtain

$$B_{i_1 j_1 i_2 j_2 i_3 j_3}^{(\text{GR})} = -\frac{32}{a^3 M_{\text{Pl}}^4} \mathcal{I}^{(\text{GR})}(k_1, k_2, k_3; \tau) \mathcal{E}_{i_1 j_1 i_2 j_2 i_3 j_3}^{(\text{GR})}(\hat{\mathbf{k}}_1, \hat{\mathbf{k}}_2, \hat{\mathbf{k}}_3), \quad (3.8)$$

$$B_{i_1 j_1 i_2 j_2 i_3 j_3}^{(\text{mass})} = \frac{192}{a^3 M_{\text{Pl}}^4} \mathcal{I}^{(\text{mass})}(k_1, k_2, k_3; \tau) \mathcal{E}_{i_1 j_1 i_2 j_2 i_3 j_3}^{(\text{mass})}(\hat{\mathbf{k}}_1, \hat{\mathbf{k}}_2, \hat{\mathbf{k}}_3), \quad (3.9)$$

where $\mathcal{I}^{(X)}$ are basically time integrals of the mode functions,

$$\mathcal{I}^{(\text{GR})}(k_1, k_2, k_3; \tau) \equiv k_1^2 \int_{-\infty}^{\tau} d\eta a^{-1}(\eta) \text{Im} [v_{k_1}^*(\tau) v_{k_2}^*(\tau) v_{k_3}^*(\tau) v_{k_1}(\eta) v_{k_2}(\eta) v_{k_3}(\eta)], \quad (3.10)$$

$$\mathcal{I}^{(\text{mass})}(k_1, k_2, k_3; \tau) \equiv \int_{-\infty}^{\tau} d\eta a(\eta) g(\eta) \text{Im} [v_{k_1}^*(\tau) v_{k_2}^*(\tau) v_{k_3}^*(\tau) v_{k_1}(\eta) v_{k_2}(\eta) v_{k_3}(\eta)], \quad (3.11)$$

while $\mathcal{E}^{(X)}$ are combinations of the tensor polarizations,

$$\begin{aligned} \mathcal{E}_{i_1 j_1 i_2 j_2 i_3 j_3}^{(\text{GR})}(\hat{\mathbf{k}}_1, \hat{\mathbf{k}}_2, \hat{\mathbf{k}}_3) &= \left[\Pi_{i_1 j_1, ij}(\hat{\mathbf{k}}_1) \Pi_{i_2 j_2, kl}(\hat{\mathbf{k}}_2) \left(\kappa_{3j} \kappa_{3l} \Pi_{i_3 j_3, ik}(\hat{\mathbf{k}}_3) - \frac{1}{2} \kappa_{3i} \kappa_{3j} \Pi_{i_3 j_3, kl}(\hat{\mathbf{k}}_3) \right) \right. \\ &\quad \left. + 5 \text{ permutation terms w.r.t. } 1, 2, 3 \right], \end{aligned} \quad (3.12)$$

$$\mathcal{E}_{i_1 j_1 i_2 j_2 i_3 j_3}^{(\text{mass})}(\hat{\mathbf{k}}_1, \hat{\mathbf{k}}_2, \hat{\mathbf{k}}_3) = \Pi_{i_1 j_1, ij}(\hat{\mathbf{k}}_1) \Pi_{i_2 j_2, jk}(\hat{\mathbf{k}}_2) \Pi_{i_3 j_3, ki}(\hat{\mathbf{k}}_3) \quad (3.13)$$

with

$$\boldsymbol{\kappa}_i \equiv \frac{\mathbf{k}_i}{k_1} \quad (i = 2, 3), \quad \Pi_{ij, kl}(\hat{\mathbf{k}}) \equiv \sum_{\lambda} e_{ij}^{\lambda}(\hat{\mathbf{k}}) e_{kl}^{*\lambda}(\hat{\mathbf{k}}). \quad (3.14)$$

We shall also adopt the notation $\kappa_i \equiv |\boldsymbol{\kappa}_i| = k_i/k_1$.

In what follows in this section, we will evaluate $\mathcal{I}^{(X)}$. As discussed in appendix B, it can be shown that $\mathcal{I}^{(X)}$ are well approximated by

$$\mathcal{I}^{(\text{GR})}(\tau) \simeq \text{Im} [v_{k_1}^*(\tau) v_{k_2}^*(\tau) v_{k_3}^*(\tau)] k_1^2 \int_{-\infty}^{\tau} d\eta a^{-1}(\eta) \text{Re} [v_{k_1}(\eta) v_{k_2}(\eta) v_{k_3}(\eta)], \quad (3.15)$$

$$\mathcal{I}^{(\text{mass})}(\tau) \simeq \text{Im} [v_{k_1}^*(\tau) v_{k_2}^*(\tau) v_{k_3}^*(\tau)] \int_{-\infty}^{\tau} d\eta a(\eta) g(\eta) \text{Re} [v_{k_1}(\eta) v_{k_2}(\eta) v_{k_3}(\eta)]. \quad (3.16)$$

We will evaluate these time integrals and the prefactor $\text{Im}[v_{k_1}^* v_{k_2}^* v_{k_3}^*]$ in Sec. 3.1 and 3.2, respectively.

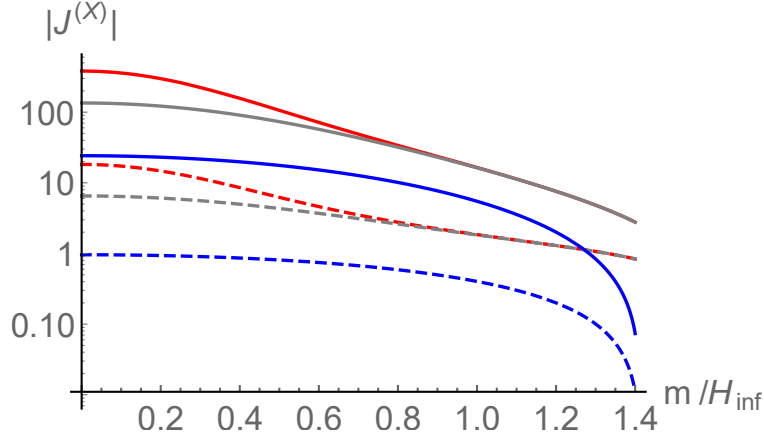


Figure 1. The numerical results of $|\mathcal{J}^{(X)}(\kappa_2, \kappa_3)|$ defined in Eq. (3.18) with $X = \text{GR}$ (blue) and $X = \text{mass}$ (red and grey) are shown as functions of m/H_{inf} . The solid and dashed line denote the squeezed configuration ($\kappa_2 = 1, \kappa_3 = 0.1$) and the equilateral configuration ($\kappa_2 = \kappa_3 = 1$), respectively. The lower bound of the integral range of $|\mathcal{J}^{(\text{mass})}|$ is $|k\tau_r| = 10^{-15}$ (red) and 10^{-5} (grey), while $|\mathcal{J}^{(\text{GR})}|$ (blue) does not depend on it. $|\mathcal{J}^{(\text{mass})}|$ is amplified for $m/H_{\text{inf}} \lesssim 0.7$ as $|k\tau_r|$ decreases.

3.1 Evaluating time integral during inflation

Concentrating on the inflationary era, $\tau < \tau_r$, one can rewrite the time integrals in Eqs. (3.15) and (3.16) as

$$\int_{-\infty}^{\tau_r} d\eta a^{\mp 1}(\eta) \text{Re} [v_{k_1}(\eta)v_{k_2}(\eta)v_{k_3}(\eta)] = \frac{\pi^{3/2}}{8k_1^{5/2}} \left(\frac{H_{\text{inf}}}{k_1} \right)^{\pm 1} \mathcal{J}^{(\text{GR}/\text{mass})}, \quad (3.17)$$

with dimensionless integrals

$$\mathcal{J}^{(\text{GR}/\text{mass})}(\kappa_2, \kappa_3) \equiv \int_{|k_1\tau_r|}^{\infty} dy y^{\frac{3}{2} \pm 1} \text{Re} \left[H_\nu^{(1)}(y) H_\nu^{(1)}(\kappa_2 y) H_\nu^{(1)}(\kappa_3 y) \right], \quad (3.18)$$

where $g(\eta)$ is assumed to be constant during inflation and $y \equiv -k_1\eta$ is introduced as a new dummy variable. $\mathcal{J}^{(\text{GR}/\text{mass})}$ depends on κ_2, κ_3 and $\nu = \sqrt{9/4 - m^2/H_{\text{inf}}^2}$ and should be numerically evaluated. In Fig. 1, we show their dependence on m/H_{inf} for the equilateral ($\kappa_2 = \kappa_3 = 1$) and the squeezed ($\kappa_3 \ll \kappa_2 = 1$) configurations. The following three observations are found in Fig. 1: (i) $|\mathcal{J}^{(\text{mass})}|$ is always larger than $|\mathcal{J}^{(\text{GR})}|$. (ii) The squeezed configuration (solid) is larger than the equilateral configuration (dashed). (iii) $|\mathcal{J}^{(\text{mass})}|$ increases as $|k\tau_r|$ decreases for $|k\tau_r| \lesssim 0.7$, while $|\mathcal{J}^{(\text{GR})}|$ is insensitive to $|k\tau_r| \ll 1$.

Comparing $\mathcal{I}^{(\text{mass})}$ and $\mathcal{I}^{(\text{GR})}$, we find

$$\frac{\mathcal{I}^{(\text{mass})}}{\mathcal{I}^{(\text{GR})}} = \frac{g_{\text{inf}}}{H_{\text{inf}}^2} \frac{\mathcal{J}^{(\text{mass})}}{\mathcal{J}^{(\text{GR})}}, \quad (3.19)$$

where g_{inf} is the value of g during inflation. Since $\mathcal{J}^{(\text{mass})}$ is larger than $\mathcal{J}^{(\text{GR})}$ by almost an order of magnitude as seen in Fig. 1, we expect that the contribution to the tensor bispectrum is dominated by $B_{i_1 j_1 i_2 j_2 i_3 j_3}^{(\text{mass})}$ rather than $B_{i_1 j_1 i_2 j_2 i_3 j_3}^{(\text{GR})}$, if $g_{\text{inf}} \gtrsim H_{\text{inf}}^2$. We will explicitly confirm this expectation with numerical computations in the next section.

One can also see in Fig. 1 that the squeezed configuration case is much larger than the equilateral case. We find that $\mathcal{J}^{(\text{GR}/\text{mass})}$ diverges in the squeezed limit as

$$\begin{aligned} \lim_{\kappa_2 \rightarrow 1, \kappa_3 \rightarrow 0} \mathcal{J}^{(\text{GR}/\text{mass})} &\simeq - \lim_{\kappa_3 \rightarrow 0} \int_{|k_1 \tau_r|}^{\infty} dy y^{\frac{3}{2} \pm 1} \text{Im} \left[\left(H_\nu^{(1)}(y) \right)^2 \right] \text{Im} \left[H_\nu^{(1)}(\kappa_3 y) \right] \\ &= \lim_{\kappa_3 \rightarrow 0} \kappa_3^{-\nu} \times \left(\frac{2^\nu \Gamma(\nu)}{\pi} \int_{|k_1 \tau_r|}^{\infty} dy y^{\frac{3}{2} - \nu \pm 1} \text{Im} \left[\left(H_\nu^{(1)}(y) \right)^2 \right] \right). \end{aligned} \quad (3.20)$$

This implies that the tensor bispectrum peaks at the squeezed configuration, and the degree of divergence in the squeezed limit is solely determined by $\nu = \sqrt{9/4 - m^2/H_{\text{inf}}^2}$.

Although $\mathcal{J}^{(\text{GR})}$ is not sensitive to the lower limit of the integral, $|k_1 \tau_r| \ll 1$, we found $\mathcal{J}^{(\text{mass})}$ depends on it for $m/H_{\text{inf}} \lesssim 0.7$. Well after all the modes with k_1, k_2, k_3 exit the horizon, the integrand of $\mathcal{J}^{(\text{GR}/\text{mass})}$ in Eq. (3.18) evolve as,

$$y^{\frac{3}{2} \pm 1} \text{Re} \left[H_\nu^{(1)}(y) H_\nu^{(1)}(\kappa_2 y) H_\nu^{(1)}(\kappa_3 y) \right] \sim y^{\frac{3}{2} - \nu \pm 1}. \quad (3.21)$$

Hence, the massless limit ($\nu = 3/2$) of $\mathcal{J}^{(\text{mass})}$ exhibits a logarithmic enhancement. Indeed, we can explicitly calculate $\mathcal{J}^{(\text{mass})}$ in the massless limit as

$$\lim_{m \rightarrow 0} \mathcal{J}^{(\text{mass})} = (1 + \kappa_2^3 + \kappa_3^3) (N_{k_1} - \gamma_E) + \frac{1}{3} (1 + \kappa_2 + \kappa_3) (4 + 4\kappa_2^2 + 4\kappa_3^2 - \kappa_2 - \kappa_3 - \kappa_2 \kappa_3), \quad (3.22)$$

where $N_{k_1} \equiv -\log |k_1 \tau_r|$ and γ_E is Euler's constant.⁶ Nevertheless, in this paper, we focus on the cases of $m/H_{\text{inf}} = \mathcal{O}(1)$ with which we obtain the amplified blue-tilted GW power spectrum, Eq. (2.10). Then, not only $\mathcal{J}^{(\text{GR})}$ but also $\mathcal{J}^{(\text{mass})}$ becomes constant for a sufficiently small $|k_1 \tau_r|$. Therefore, we can ignore the late time contribution to $\mathcal{J}^{(\text{GR}/\text{mass})}$.

3.2 Evolution after inflation

Now we consider the factor $\text{Im} [v_{k_1}^*(\tau) v_{k_2}^*(\tau) v_{k_3}^*(\tau)]$ in Eqs. (3.15) and (3.16) which represents the post-inflationary evolution of the bispectrum. Evaluating at the end of inflation and using eq. (2.7) again, one finds

$$a^{-3}(\tau_r) \text{Im} [v_{k_1}^*(\tau_r) v_{k_2}^*(\tau_r) v_{k_3}^*(\tau_r)] \simeq \frac{2^{3\nu-3} \Gamma^3(\nu) H_{\text{inf}}^3}{\pi^{3/2} \kappa_2^\nu \kappa_3^\nu k_1^{9/2}} |k_1 \tau_r|^{\frac{3}{2}(3-2\nu)}, \quad (3.23)$$

where a^{-3} was multiplied because the bispectrum has this prefactor in Eqs. (3.8) and (3.9) which originally comes from the fact, $h(\tau) \propto v(\tau)/a(\tau)$. The evolution after inflation is given by a factor from Eqs. (2.9) and (2.12)

$$\frac{v_k(\tau)}{v_k(\tau_r)} = \sqrt{\frac{\tau_m}{\tau_r}} \gamma_k \frac{a(\tau)}{a(\tau_r)} \mathcal{T}_k(\tau). \quad (3.24)$$

Now we obtain

$$a^{-3}(\tau) \text{Im} [v_{k_1}^*(\tau) v_{k_2}^*(\tau) v_{k_3}^*(\tau)] \simeq H_{\text{inf}}^3 \frac{\mathcal{T}_{k_1}(\tau) \mathcal{T}_{k_2}(\tau) \mathcal{T}_{k_3}(\tau)}{2^{3/2} \kappa_2^\nu \kappa_3^\nu k_1^{9/2}} \tilde{\gamma}_{k_1} \tilde{\gamma}_{k_2} \tilde{\gamma}_{k_3} \left[|k_1 \tau_r|^{(3-2\nu)} \frac{\tau_m}{\tau_r} \right]^{\frac{3}{2}}. \quad (3.25)$$

⁶Basically this integral was calculated in Ref. [34] (see Eq. (72) of the paper). There are, however, a couple of typos in the paper including the absence of the term proportional to N_{k_1} . For these points, we contacted the authors of Ref. [34] and we have got the agreement.

Here, the last factor $\tilde{\gamma}_{k_1}\tilde{\gamma}_{k_2}\tilde{\gamma}_{k_3} [|k_1\tau_r|^{(3-2\nu)}\tau_m/\tau_r]^{3/2}$ reminds us of the expression for the power spectrum, Eq. (2.10). Since the power spectrum ($\propto h^2$) gains the factor $\tilde{\gamma}_k^2 |k_1\tau_r|^{(3-2\nu)}\tau_m/\tau_r$, it is reasonable for the bispectrum ($\propto h^3$) to acquire it to the 3/2 power.

In the case of the instant reheating, the transfer function for the massless tensor at the present time $\mathcal{T}_k(\tau_0)$ is given by [59]

$$\mathcal{T}_k(\tau_0) = \Omega_{m0} \sqrt{\frac{g_*(T_{\text{in}})}{g_{*0}}} \left(\frac{g_{*s0}}{g_{*s}(T_{\text{in}})} \right)^{2/3} \frac{3j_1(k\tau_0)}{k\tau_0} \tilde{T}_1(k/k_{\text{eq}}), \quad (3.26)$$

where $j_1(x) = (\sin(x)/x - \cos(x))/x$, $\tilde{T}_1(x) = 1 + 1.57x + 3.42x^2$, T_{in} is the temperature of the universe when the mode reenters the horizon and $k_{\text{eq}} = 7.1 \times 10^{-2} \Omega_{m0} h^2 \text{Mpc}^{-1}$ is the wavenumber corresponding to the horizon scale of the matter-radiation equality.

3.3 Tensor bispectrum today

Putting the results of the previous subsections altogether, we obtain the two contributions to the contracted bispectrum at the present time as

$$k_1^2 k_2^2 k_3^2 B_h^{(\text{GR})} = -\frac{1}{2} (2\pi)^{3/2} \frac{H_{\text{inf}}^4}{M_{\text{Pl}}^4} \frac{\mathcal{E}^{(\text{GR})} \mathcal{J}^{(\text{GR})}}{\kappa_2^{\nu-2} \kappa_3^{\nu-2}} \mathcal{T}_{k_1} \mathcal{T}_{k_2} \mathcal{T}_{k_3}(\tau_0) \tilde{\gamma}_{k_1} \tilde{\gamma}_{k_2} \tilde{\gamma}_{k_3} \left[|k_1\tau_r|^{(3-2\nu)} \frac{\tau_m}{\tau_r} \right]^{\frac{3}{2}}, \quad (3.27)$$

$$k_1^2 k_2^2 k_3^2 B_h^{(\text{mass})} = 3(2\pi)^{3/2} \frac{g_{\text{inf}} H_{\text{inf}}^2}{M_{\text{Pl}}^4} \frac{\mathcal{E}^{(\text{mass})} \mathcal{J}^{(\text{mass})}}{\kappa_2^{\nu-2} \kappa_3^{\nu-2}} \mathcal{T}_{k_1} \mathcal{T}_{k_2} \mathcal{T}_{k_3}(\tau_0) \tilde{\gamma}_{k_1} \tilde{\gamma}_{k_2} \tilde{\gamma}_{k_3} \left[|k_1\tau_r|^{(3-2\nu)} \frac{\tau_m}{\tau_r} \right]^{\frac{3}{2}}, \quad (3.28)$$

where we multiplied $B_h^{(\text{GR}/\text{mass})}$ by $(k_1 k_2 k_3)^2$ in order to make them dimensionless. Here, the contracted polarization tensors $\mathcal{E}^{(\text{GR}/\text{mass})} \equiv \delta_{j_1 i_2} \delta_{j_2 i_3} \delta_{j_3 i_1} \mathcal{E}_{i_1 j_1 i_2 j_2 i_3 j_3}^{(\text{GR}/\text{mass})}$ are computed as

$$\mathcal{E}^{(\text{GR})} = \frac{1}{1024 \kappa_2^4 \kappa_3^4} \left(\kappa_2^4 - 2\kappa_2^2 (\kappa_3^2 + 1) + (\kappa_3^2 - 1)^2 \right)^2 \left[\kappa_2^6 + 15\kappa_2^4 (\kappa_3^2 + 1) + 15\kappa_2^2 (\kappa_3^4 + 6\kappa_3^2 + 1) + (\kappa_3^6 + 15\kappa_3^4 + 15\kappa_3^2 + 1) \right], \quad (3.29)$$

$$\mathcal{E}^{(\text{mass})} = \frac{1}{512 \kappa_2^4 \kappa_3^4} \left(-2(\kappa_2^2 + 1)\kappa_3^2 + (\kappa_2^2 - 1)^2 + \kappa_3^4 \right)^2 \left(\kappa_2^4 + 6\kappa_2^2 (\kappa_3^2 + 1) + \kappa_3^4 + 6\kappa_3^2 + 1 \right). \quad (3.30)$$

For instance, their values at the squeezed and equilateral configurations are

$$\mathcal{E}^{(\text{GR})} = \frac{1}{2}, \quad \mathcal{E}^{(\text{mass})} = \frac{1}{4}. \quad (\text{Squeezed : } \kappa_2 = 1, \kappa_3 \rightarrow 0) \quad (3.31)$$

$$\mathcal{E}^{(\text{GR})} = \frac{1647}{1024}, \quad \mathcal{E}^{(\text{mass})} = \frac{189}{512}. \quad (\text{Equilateral : } \kappa_2 = \kappa_3 = 1) \quad (3.32)$$

We can also define their shape functions as

$$S^{(\text{X})}(\kappa_2, \kappa_3) = \mathcal{N}^{(\text{X})} \kappa_2^{2-\nu} \kappa_3^{2-\nu} \mathcal{E}^{(\text{X})}(\kappa_2, \kappa_3) \mathcal{J}^{(\text{X})}(\kappa_2, \kappa_3), \quad (\text{X} = \text{GR}/\text{mass}) \quad (3.33)$$

where the factor $\mathcal{N}^{(\text{X})} = [\mathcal{E}^{(\text{X})} \mathcal{J}^{(\text{X})}(\kappa_2 = \kappa_3 = 1)]^{-1}$ normalizes the shape function at the equilateral configuration such that $S^{(\text{X})}(\kappa_2 = \kappa_3 = 1) = 1$. From Eq. (3.20), one finds that

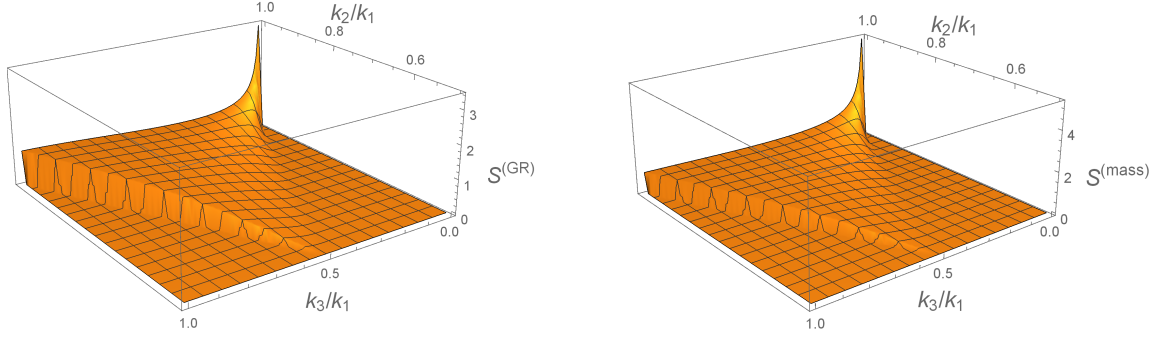


Figure 2. The shape functions $S^{(\text{GR})}$ (left panel) and $S^{(\text{mass})}$ (right panel) defined in Eq. (3.33) are shown for $m/H_{\text{inf}} = 0.8$. Both of them diverge at the squeezed limit, $\kappa_2 \rightarrow 1$ and $\kappa_3 \rightarrow 0$.

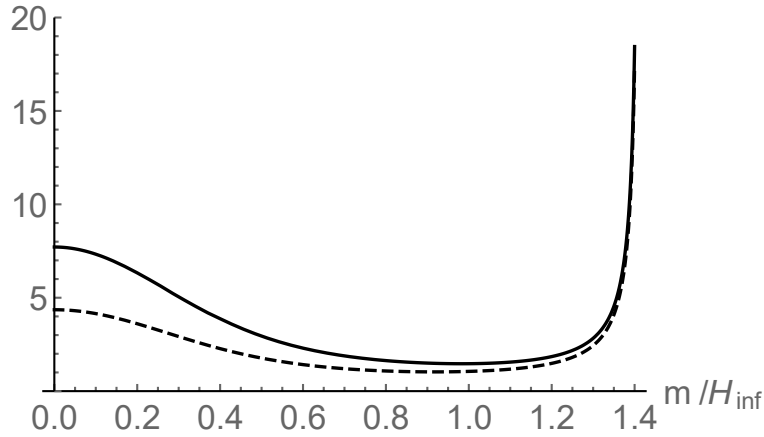


Figure 3. $|\mathcal{E}^{(\text{mass})} \mathcal{J}^{(\text{mass})} / \mathcal{E}^{(\text{GR})} \mathcal{J}^{(\text{GR})}|$ which appears in the ratio $|B_h^{(\text{mass})} / B_h^{(\text{GR})}|$ in Eq. (3.35) is plotted for $0 \leq m/H_{\text{inf}} \leq 1.4$. The solid and dashed line denote the squeezed configuration ($\kappa_2 = 1, \kappa_3 = 0.1$) and the equilateral configuration ($\kappa_2 = \kappa_3 = 1$), respectively. This plot implies that $|\mathcal{E}^{(\text{mass})} \mathcal{J}^{(\text{mass})} / \mathcal{E}^{(\text{GR})} \mathcal{J}^{(\text{GR})}|$ is always larger than unity.

the asymptotic behavior of the shape functions in the squeezed limit is the same for the two contributions,

$$\lim_{\kappa_2 \rightarrow 1, \kappa_3 \rightarrow 0} S^{(X)}(\kappa_2, \kappa_3) \propto \kappa_3^{2-2\nu}, \quad (X = \text{GR}/\text{mass}) \quad (3.34)$$

and $(k_1 k_2 k_3)^2 B_h$ diverges in the squeezed limit for $\nu > 1 \iff m/H_{\text{inf}} < \sqrt{5}/2 \approx 1.12$.

Let us compare the amplitudes of the two contributions, $B_h^{(\text{mass})}$ and $B_h^{(\text{GR})}$. Their ratio is given by

$$\left| \frac{B_h^{(\text{mass})}}{B_h^{(\text{GR})}} \right| = 6 \frac{g_{\text{inf}}}{H_{\text{inf}}^2} \left| \frac{\mathcal{E}^{(\text{mass})} \mathcal{J}^{(\text{mass})}}{\mathcal{E}^{(\text{GR})} \mathcal{J}^{(\text{GR})}} \right| \gtrsim 6 \frac{g_{\text{inf}}}{H_{\text{inf}}^2}. \quad (3.35)$$

Here, $|\mathcal{E}^{(\text{mass})} \mathcal{J}^{(\text{mass})} / \mathcal{E}^{(\text{GR})} \mathcal{J}^{(\text{GR})}|$ is plotted in Fig. 3 and is shown to be larger than unity irrespective of m/H_{inf} or configuration. Therefore, for $g_{\text{inf}}/H_{\text{inf}}^2 = \mathcal{O}(1)$, the new contribution to the bispectrum $B_h^{(\text{mass})}$ dominates the conventional one $B_h^{(\text{GR})}$.

It is interesting to note that the bispectrum divided by the square root of the power spectra can be written in a simple expression,

$$\frac{(k_1 k_2 k_3)^2 B_h(k_1, k_2, k_3)}{[\mathcal{P}_h(k_1)\mathcal{P}_h(k_2)\mathcal{P}_h(k_3)]^{1/2}} \simeq \frac{3\pi^{9/2} g_{\text{inf}}}{H_{\text{inf}} M_{\text{Pl}}} \mathcal{E}^{(\text{mass})} \mathcal{J}^{(\text{mass})} (\kappa_2 \kappa_3)^{\frac{7}{2}-2\nu}, \quad (3.36)$$

where the sub-leading contribution from $B_h^{(\text{GR})}$ is ignored. Here, the common factor discussed below Eq. (3.25) which enhances both the power spectrum and bispectrum is cancelled out.

4 Quadrupolar modulation of tensor power spectrum

In this section we discuss the detectability of the primordial tensor bispectrum calculated in the previous section. Although it seems that the simplest way to detect the tensor bispectrum is the direct measurement of it at interferometer scales, it was shown that the bispectrum cannot be probed directly [50, 51]. Instead of this, we briefly discuss the detectability based on the modulation of the tensor power spectrum induced by the squeezed tensor bispectrum.

The tensor power spectrum with polarization λ_1 modulated by a long tensor mode with polarization λ_3 and wavevector \mathbf{k}_3 is given by

$$\lim_{k_3 \rightarrow 0} \langle h_{\mathbf{k}_1}^{\lambda_1} h_{\mathbf{k}_2}^{\lambda_1} \rangle'_{h_{\mathbf{k}_3}^{\lambda_3}} \simeq \langle h_{\mathbf{k}_1}^{\lambda_1} h_{\mathbf{k}_2}^{\lambda_1} \rangle' + \lim_{k_3 \rightarrow 0} \left(h_{\mathbf{k}_3}^{\lambda_3} \frac{\langle h_{\mathbf{k}_1}^{\lambda_1} h_{\mathbf{k}_2}^{\lambda_1} h_{\mathbf{k}_3}^{\lambda_3} \rangle'}{P_h^{\lambda_3}(k_3)} \right), \quad (4.1)$$

where the prime on the expectation value $\langle \dots \rangle'$ indicates that the momentum conserving delta function and a factor of $(2\pi)^3$ are removed. Here, the power spectrum is given by

$$P_h^\lambda(k) = \frac{2H_{\text{inf}}^2}{M_{\text{Pl}}^2 k^3} \mathcal{T}_k^2(\tau_0) \tilde{\gamma}_k^2 |k\tau_r|^{(3-2\nu)} \frac{\tau_m}{\tau_r}, \quad (4.2)$$

where the two polarizations are not summed over and $P_h(k) = 2P_h^\lambda(k)$ in our model.

From the definition of tensor bispectrum shown in Eq. (3.5), one finds

$$\begin{aligned} \langle h_{\mathbf{k}_1}^{\lambda_1} h_{\mathbf{k}_2}^{\lambda_1} h_{\mathbf{k}_3}^{\lambda_3} \rangle' &= e_{ij}^{\lambda_1*}(\hat{\mathbf{k}}_1) e_{kl}^{\lambda_1*}(\hat{\mathbf{k}}_2) e_{mn}^{\lambda_3*}(\hat{\mathbf{k}}_3) B_{ijklmn}(k_1, k_2, k_3) \\ &\simeq \frac{192}{a^3 M_{\text{Pl}}^4} \mathcal{I}^{(\text{mass})} e_{ij}^{\lambda_1*}(\hat{\mathbf{k}}_1) e_{kl}^{\lambda_1*}(\hat{\mathbf{k}}_2) e_{mn}^{\lambda_3*}(\hat{\mathbf{k}}_3) \mathcal{E}_{ijklmn}^{(\text{mass})}(\hat{\mathbf{k}}_1, \hat{\mathbf{k}}_2, \hat{\mathbf{k}}_3) \\ &= \frac{192}{a^3 M_{\text{Pl}}^4} \mathcal{I}^{(\text{mass})} e_{ij}^{\lambda_1*}(\hat{\mathbf{k}}_1) e_{jk}^{\lambda_1*}(\hat{\mathbf{k}}_2) e_{ki}^{\lambda_3*}(\hat{\mathbf{k}}_3), \end{aligned} \quad (4.3)$$

where we ignored the subdominant contribution from the GR interaction in the second line. This equation can be reduced by summing over λ_1 in the squeezed limit,

$$\begin{aligned} \lim_{k_3 \rightarrow 0} \sum_{\lambda_1} \langle h_{\mathbf{k}_1}^{\lambda_1} h_{\mathbf{k}_2}^{\lambda_1} h_{\mathbf{k}_3}^{\lambda_3} \rangle' &\simeq \lim_{k_3 \rightarrow 0} \frac{-192}{a^3 M_{\text{Pl}}^4} \mathcal{I}^{(\text{mass})} e_{ij}^{\lambda_3*}(\hat{\mathbf{k}}_3) \hat{k}_1^i \hat{k}_1^j \\ &= \lim_{k_3 \rightarrow 0} \frac{-3\pi^{3/2} g_{\text{inf}}}{2H_{\text{inf}} M_{\text{Pl}} k_1^{3/2}} P_h(k_1) \sqrt{P_h^{\lambda_3}(k_3)} \mathcal{J}^{(\text{mass})} e_{ij}^{\lambda_3*}(\hat{\mathbf{k}}_3) \hat{k}_1^i \hat{k}_1^j, \end{aligned} \quad (4.4)$$

where $\sum_{\lambda} e_{ij}^{\lambda*}(\hat{\mathbf{k}}) e_{jl}^{\lambda}(\hat{\mathbf{k}}) = \delta_{il} - \hat{k}_i \hat{k}_l$ is used in the first line.

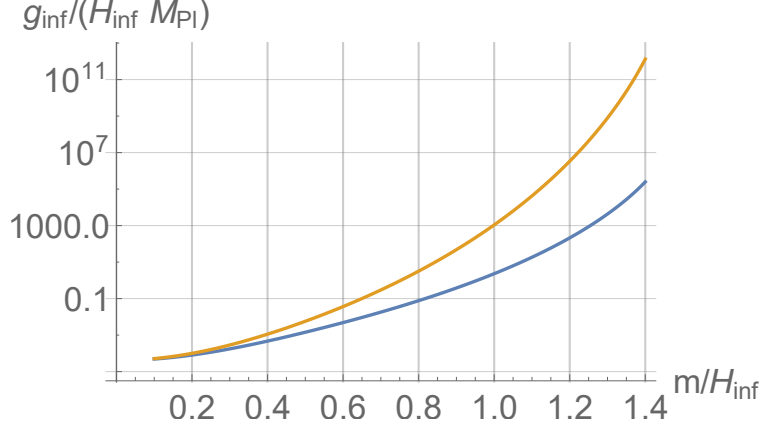


Figure 4. Plots of $g_{\text{inf}}/(H_{\text{inf}} M_{\text{Pl}})$ that gives $\sqrt{\langle \mathcal{Q} \rangle^2} = 10^{-2}$ as functions of m/H_{inf} . The color scheme is orange for $\kappa_{\text{UV}} = 10^{-15}$ and blue for $\kappa_{\text{UV}} = 10^{-8}$, which roughly correspond to LISA and SKA, respectively. The lower bound of the κ_3 integral is taken as $10^{-15} \kappa_{\text{UV}}$.

Substituting it into Eq. (4.1), the observable power spectrum taking into account the presence of the long tensor mode $h_{\mathbf{k}_3}^{\lambda_3}$ has the following quadrupole modulation

$$\begin{aligned} \lim_{k_3 \rightarrow 0} P_h(\mathbf{k}_1) \Big|_{h_{\mathbf{k}_3}^{\lambda_3}}^{(\text{obs})} &\simeq \lim_{k_3 \rightarrow 0} P_h(k_1) \left(1 + \hat{f}_{\text{NL}}^{\lambda_3}(k_3) h_{\mathbf{k}_3}^{\lambda_3} e_{ij}^{\lambda_3*}(\hat{\mathbf{k}}_3) \hat{k}_1^i \hat{k}_1^j \right) \\ &\equiv \lim_{k_3 \rightarrow 0} P_h(k_1) \left(1 + \tilde{\mathcal{Q}}_{ij}^{\lambda_3}(\mathbf{k}_3) \hat{k}_1^i \hat{k}_1^j \right), \end{aligned} \quad (4.5)$$

with

$$\hat{f}_{\text{NL}}^{\lambda_3}(k_3) \equiv \frac{-3\pi^{3/2} g_{\text{inf}}}{2H_{\text{inf}} M_{\text{Pl}} k_1^{3/2}} \frac{\mathcal{J}^{(\text{mass})}}{\sqrt{P_h^{\lambda_3}(k_3)}}. \quad (4.6)$$

Then, the observed quadrupole in the tensor power spectrum can be obtained by summing over both long-mode polarizations $\lambda_3 = \pm$ and wave vector \mathbf{k}_3 ,

$$\mathcal{Q}_{ij}(\mathbf{x}) = \lim_{k_3 \rightarrow 0} \int \frac{d^3 k_3}{(2\pi)^3} e^{i\mathbf{k}_3 \cdot \mathbf{x}} \sum_{\lambda_3} \tilde{\mathcal{Q}}_{ij}^{\lambda_3}(\mathbf{k}_3). \quad (4.7)$$

Note that the lower limit of the integral in the above equation is given by the scale corresponding to the infrared cutoff which is, however, not relevant in our case. The expectation value of the quadrupole moments squared can be calculated as

$$\begin{aligned} \langle \mathcal{Q} \rangle^2 &\equiv \frac{8\pi}{15} \langle \mathcal{Q}_{ij}(\mathbf{x}) \mathcal{Q}_{ij}(\mathbf{x}) \rangle = \lim_{k_3 \rightarrow 0} \frac{8\pi}{15} \int \frac{d^3 k_3}{(2\pi)^3} \sum_{\lambda_3} \langle \tilde{\mathcal{Q}}_{ij}^{\lambda_3*}(\mathbf{k}_3) \tilde{\mathcal{Q}}_{ij}^{\lambda_3}(\mathbf{k}_3) \rangle' \\ &= \lim_{k_3 \rightarrow 0} \frac{4}{15\pi} \int dk_3 k_3^2 \sum_{\lambda_3} \left(\hat{f}_{\text{NL}}^{\lambda_3}(k_3) \right)^2 P_h^{\lambda_3}(k_3) \\ &= \frac{6\pi^2}{5} \left(\frac{g_{\text{inf}}}{H_{\text{inf}} M_{\text{Pl}}} \right)^2 \int d\kappa_3 \kappa_3^2 \left(\mathcal{J}^{(\text{mass})} \right)^2. \end{aligned} \quad (4.8)$$

Using Eq. (3.20), this integral is evaluated as

$$\int^{\kappa_{\text{UV}}} d\kappa_3 \kappa_3^2 \left[\mathcal{J}^{(\text{mass})} \right]^2 \simeq \mathcal{G} \left(\frac{m}{H_{\text{inf}}} \right) \frac{\kappa_{\text{UV}}^{3-2\nu}}{3-2\nu}, \quad (4.9)$$

with

$$\begin{aligned} \mathcal{G} \left(\frac{m}{H_{\text{inf}}} \right) &\equiv \left(\frac{2^\nu \Gamma(\nu)}{\pi} \int_{|k_1 \tau_r|}^{\infty} dy y^{\frac{3}{2}-\nu \pm 1} \text{Im} \left[\left(H_\nu^{(1)}(y) \right)^2 \right] \right)^2 \\ &\approx \exp \left[1.80919 \left(\frac{m}{H_{\text{inf}}} \right)^3 - 2.01653 \left(\frac{m}{H_{\text{inf}}} \right)^2 - 4.96751 \left(\frac{m}{H_{\text{inf}}} \right) + 5.58025 \right], \end{aligned} \quad (4.10)$$

where κ_{UV} denotes UV cutoff of κ_3 and a numerical fit is used in the second line. It is worth mentioning that the concrete value of κ_{UV} depends on the target scale at which we expect to observe the quadrupole modulation. For example, by assuming that k_3 is slightly larger than the horizon scale today, for the scale corresponding to interferometers like LISA, $\kappa_{\text{UV}} \simeq 10^{-15}$, while for the one corresponding to pulsar timing arrays like SKA, $\kappa_{\text{UV}} \simeq 10^{-8}$.

Combining all results in this section so far, g_{inf} can be expressed as⁷

$$\frac{g_{\text{inf}}}{H_{\text{inf}} M_{\text{Pl}}} = \sqrt{\frac{5}{6\pi^2}} \sqrt{(\mathcal{Q})^2} \left(\frac{3-2\nu}{\kappa_{\text{UV}}^{3-2\nu}} \right)^{\frac{1}{2}} \mathcal{G} \left(\frac{m}{H_{\text{inf}}} \right)^{-\frac{1}{2}}, \quad (4.11)$$

According to recent discussions on the quadrupole modulation induced by the tensor bispectrum, it was suggested that the quadrupole can be observed if $\sqrt{(\mathcal{Q})^2} \gtrsim 10^{-2}$ [60, 61] on small scales, where the tensor power spectrum is observable. In Fig. 4, numerical plots of $g_{\text{inf}}/(H_{\text{inf}} M_{\text{Pl}})$ that give $\sqrt{(\mathcal{Q})^2} = 10^{-2}$ are shown. If the value of g_{inf} for given m/H_{inf} is greater than the one shown by the plots, the modulation can be probed at the interferometer scale (the orange plot with $\kappa_{\text{UV}} = 10^{-15}$) or the scale of pulsar timing arrays (the blue plot with $\kappa_{\text{UV}} = 10^{-8}$).

Making use of the expression (4.11), the dependence of $g_{\text{inf}}/(H_{\text{inf}} M_{\text{Pl}})$ on κ_{UV} and m/H_{inf} can be understood as follows. For a fixed m/H_{inf} , its power on κ_{UV} is $-3/2 + \nu$ that is negative for $0 < \nu < 3/2$. Then, for κ_{UV} that is positive and much smaller than 1, a larger $g_{\text{inf}}/(H_{\text{inf}} M_{\text{Pl}})$ is required for the detectability with a smaller κ_{UV} . On the other hand, for a fixed κ_{UV} , from the second line of (4.10), we can show that $(\mathcal{G}(m/H_{\text{inf}}))^{-1/2}$ is an increasing function of m/H_{inf} for the region shown in Fig. 4, which means that a larger $g_{\text{inf}}/(H_{\text{inf}} M_{\text{Pl}})$ is required for the detectability with a larger m/H_{inf} . Qualitatively, both of these features can be explained by the fact that the tensor power spectrum is blue-tilted, where the effect of the super horizon mode crucial for the modulation is suppressed for smaller κ_{UV} with fixed m/H_{inf} or for larger m/H_{inf} with fixed κ_{UV} . Then, for large m/H_{inf} , the detectability requires a very large value of $g_{\text{inf}}/(H_{\text{inf}} M_{\text{Pl}})$, which needs an enormous fine-tuning, but for small m/H_{inf} , we do not need such a fine-tuning. For example, for $m/H_{\text{inf}} = 0.5$, which still

⁷For the present case with $m/H_{\text{inf}} = \mathcal{O}(1)$, a theoretically natural choice for the value of g_{inf} would be of order $\mathcal{O}(H_{\text{inf}}^2)$, which can be different from $\mathcal{O}(H_{\text{inf}} M_{\text{Pl}})$. Moreover, theoretical considerations such as the positivity bound may lead to some constraints on the range of g_{inf} . However, in the present paper, we instead adopt the purely phenomenological standpoint and discuss the interesting range of g_{inf} for on-going/future experiments. For this purpose it is convenient to put bounds on g_{inf} in the unit of $H_{\text{inf}} M_{\text{Pl}}$ instead of H_{inf}^2 , assuming that H_{inf} is not too different from M_{Pl} .

gives interesting results on the tensor power spectrum [16], in order to obtain $\sqrt{(\mathcal{Q})^2} \gtrsim 10^{-2}$, observable at the interferometer scale, we just need

$$\frac{g_{\text{inf}}}{H_{\text{inf}} M_{\text{Pl}}} \gtrsim 10^{-2}. \quad (4.12)$$

5 Conclusions and Discussions

Recently, based on the minimal theory of massive gravity (MTMG), we proposed a new scenario predicting blue-tilted and largely amplified primordial gravitational waves (GWs) [16]. In the scenario, the primordial GWs can be detected by interferometer experiments, even if their signal is not observed at the CMB scale. While the analysis in Ref. [16] was limited to the linear perturbation related with the tensor power spectrum, since there are many other possible sources producing the GWs detectable at the interferometer scales, it is important to clarify how to distinguish our scenario from others. In this paper, as a natural extension of the previous analysis, we have considered the non-Gaussianity of primordial GWs in the scenario with the special emphasis on the tensor bispectrum.

We have shown that in MTMG, the interaction Hamiltonian for the tensor perturbation at the third order has two contributions, where one has the same form as the usual one derived from general relativity (GR) and the other is peculiar to MTMG. With this interaction Hamiltonian, we have calculated the tensor bispectrum based on the in-in formalism. Our method to obtain the tensor bispectrum today can be separated into the following two steps. The first step is evaluating the time integral in the in-in formalism during inflation. At this step, since the form of the interaction Hamiltonian peculiar to MTMG is the same as the one appearing in supersolid inflation, the calculation of this part itself is not new, while we have presented new results for the parameter region with the graviton mass comparable to the Hubble expansion rate during inflation. The second step is taking into account the enhancement of the GWs after inflation that is crucial in our scenario and is new. Combing these together, we have found that the contribution from the three-point interaction peculiar to MTMG dominates the one derived from GR and that the resultant tensor bispectrum peaks at the squeezed limit whose slope is determined by the graviton mass.

We have also considered the detectability of this tensor bispectrum. Since it had been shown in the literature that the bispectrum cannot be probed directly at interferometer scales, we have instead discussed the detectability based on the quadrupolar modulation of the tensor power spectrum, which is induced by the squeezed tensor bispectrum, making use of the well-known idea of the tensor fossils. We have shown that for $m/H_{\text{inf}} = 0.5$, which is sufficient to generate a blue-tilted and amplified tensor power spectrum detectable at the interferometer scales, if g_{inf} , the coefficient of the three-point interaction peculiar to MTMG with the dimension of mass squared, is larger than $10^{-2} H_{\text{inf}} M_{\text{Pl}}$, which is natural for H_{inf} not so smaller than M_{Pl} , the quadrupolar modulation sourced by the squeezed tensor bispectrum is observable.

The appearance of the quadrupolar modulation of the tensor power spectrum is related with the Maldacena's consistency relation on the squeezed limit of the tensor three-point function [36] with which it was shown that tensor modes with wavelengths much longer than the present Hubble radius are unobservable [62]. Actually, for the setup of solid inflation, in Ref. [63], it was shown that the appearance of the quadrupolar modulation is related with

the fact that the Maldacena’s consistency relation is violated in the model [64, 65].⁸ It is interesting to see if the consistency relation is violated or not in the scenario we considered whose setup can be regarded as generalization of solid inflation, explicitly.

In this paper, we have restricted ourselves to the case where the massive graviton is the only spin-2 particle. On the other hand, recently, from the viewpoint of cosmological collider [68, 69], the possibility that there are extra new particles in the very high energy regime like during inflation has been actively explored. Although most of works so far are intended to find particles with spin less than 2, some phenomenology is investigated for the case with extra spin-2 particles [60, 70–78]. The generalization of the current work to this direction might be worth investigating.

Finally, in this paper, as an extension of [16], where the amplitude of tensor power spectrum is large at the interferometer scales, but small at the CMB scale, we have not considered the possibility that the tensor bispectrum in this model is detectable by on-going CMB experiments. However, for some parameter region, it is possible that the amplitude of the tensor bispectrum is sufficiently large at the CMB scale, while that of the tensor power spectrum is not. So far, the detectability of tensor bispectra by CMB experiments are discussed for only very limited types of the tensor bispectra whose forms are well approximated by given templates (see [79], for a review) and the tensor bispectrum generated in our model does not fall into such classes. Therefore, it might be also interesting to consider the detectability of the tensor bispectrum in this model by CMB experiments. We would like to leave these topics for future work.

Acknowledgments

We would like to thank E. Dimastrogiovanni, P. Creminelli, M. Fasiello, S. Koroyanagi, V. De Luca, G. Franciolini, A. Ricciardone and G. Tasinato for useful discussions. The work of TF was supported by JSPS KAKENHI No. 17J09103 and No. 18K13537. The work of SMi was supported by JSPS KAKENHI No. 16K17709. The work of SMu was supported by JSPS KAKENHI No. 17H02890, No. 17H06359 and also partially supported by the World Premier International Research Center Initiative (WPI Initiative), MEXT, Japan.

A Graviton mass and coupling constant in MTMG Theory

In the main text, we have studied primordial tensor non-Gaussianity from massive gravity which predicts blue-tilted and largely amplified gravitational waves without relying on details of a concrete theory. On the other hand, MTMG [20, 21], which has a mass scale m and three dimensionless parameters c_i ($i = 1, 2, 3$), is a concrete example giving such interesting phenomenology. Therefore, here, we express the tensor graviton mass μ and coupling constant g in terms of the parameters in MTMG. The FLRW cosmology in this theory has two branches of solutions, the self-accelerating branch and the normal branch. In the self-accelerating branch, the effective cosmological constant is given by

$$\Lambda_{\text{eff}} = \frac{m^2}{2} X(c_1 X^2 + 3c_2 X + c_3), \quad (\text{A.1})$$

⁸For recent discussions on the implication of the violation of Maldacena’s consistency relation in solid inflation, see [66, 67].

where X is a constant satisfying $c_1 X^2 + 2c_2 X + c_3 = 0$. In this set-up, it was shown that the squared mass of graviton is given by

$$\mu^2 = \frac{m^2}{2} X \left[c_2 X + c_3 + \frac{H}{H_f} (c_1 X + c_2) \right], \quad (\text{A.2})$$

where H_f is the Hubble expansion rate of the fiducial metric and it can be freely specified. The self-coupling constant of the cubic interaction is given by

$$g = -\frac{m^2}{24} X \left[c_2 X - c_3 + \frac{H}{H_f} (c_1 X - c_2) \right]. \quad (\text{A.3})$$

B Real Part versus Imaginary Part

In this section, we derive the approximation in Eqs. (3.15) and (3.16). The integrals in Eqs. (3.10) and (3.11) are evaluated at the end of inflation as

$$\int_{-\infty}^{\tau_r} d\eta a^{\mp 1}(\eta) \text{Im} [v_{k_1}^*(\tau) v_{k_2}^*(\tau) v_{k_3}^*(\tau) v_{k_1}(\eta) v_{k_2}(\eta) v_{k_3}(\eta)] = \mathcal{I}_{\text{im}} + \mathcal{I}_{\text{re}}, \quad (\text{B.1})$$

with

$$\begin{aligned} \mathcal{I}_{\text{im}} &= \text{Im} [v_{k_1}^*(\tau_r) v_{k_2}^*(\tau_r) v_{k_3}^*(\tau_r)] \int_{-\infty}^{\tau_r} d\eta a^{\mp 1}(\eta) \text{Re} [v_{k_1}(\eta) v_{k_2}(\eta) v_{k_3}(\eta)], \\ \mathcal{I}_{\text{re}} &= \text{Re} [v_{k_1}^*(\tau_r) v_{k_2}^*(\tau_r) v_{k_3}^*(\tau_r)] \int_{-\infty}^{\tau_r} d\eta a^{\mp 1}(\eta) \text{Im} [v_{k_1}(\eta) v_{k_2}(\eta) v_{k_3}(\eta)]. \end{aligned} \quad (\text{B.2})$$

Since its integrand increases in time, \mathcal{I}_{re} is analytically performed with the super-horizon asymptotic form of the mode function as

$$\begin{aligned} \mathcal{I}_{\text{re}} &= \text{Re} [v_{k_1}^*(\tau_r) v_{k_2}^*(\tau_r) v_{k_3}^*(\tau_r)] \int_{-\infty}^{\tau_r} d\eta a^{\mp 1}(\eta) \text{Im} [v_{k_1}(\eta) v_{k_2}(\eta) v_{k_3}(\eta)] \\ &= \text{Re} [v_{k_1}^*(\tau_r) v_{k_2}^*(\tau_r) v_{k_3}^*(\tau_r)] \frac{2^{3(\nu-1)} \Gamma^3(\nu)}{\pi^{3/2} k_1^{5/2} (\kappa_2 \kappa_3)^\nu} \left(\frac{k_1}{H_{\text{inf}}} \right)^{\mp 1} \int_{|k_1 \tau_r|}^{\infty} dy y^{\frac{3}{2} \pm 1 - 3\nu} \\ &\simeq \text{Im} [v_{k_1}^*(\tau_r) v_{k_2}^*(\tau_r) v_{k_3}^*(\tau_r)] \frac{2^{2\nu-3} \pi^{3/2} \Gamma^2(\nu)}{k_1^{5/2} (\kappa_2 \kappa_3)^\nu \Gamma(\nu+1)} \frac{|k_1 \tau_r|^{\frac{5}{2}-\nu}}{\frac{5}{2} \mp 1 - 3\nu} a_r^{\mp 1} (1 + \kappa_2^{2\nu} + \kappa_3^{2\nu}), \end{aligned} \quad (\text{B.3})$$

where $m/H_{\text{inf}} < 0.94$ is assumed to simplify $\int dy y^{-3\nu+5/2}$. Using Eq. (3.17), one finds

$$\frac{\mathcal{I}_{\text{re}}}{\mathcal{I}_{\text{im}}} \simeq \frac{2^{2\nu} \Gamma^2(\nu) (1 + \kappa_2^{2\nu} + \kappa_3^{2\nu})}{\Gamma(\nu+1) (\kappa_2 \kappa_3)^\nu \mathcal{J}^{(\text{GR/mass})}} \frac{|k_1 \tau_r|^{\frac{5}{2}-\nu \pm 1}}{\frac{5}{2} \mp 1 - 3\nu}. \quad (\text{B.4})$$

The factor $|k_1 \tau_r|^{\frac{5}{2}-\nu \pm 1}$ is tiny in the massive case. Therefore, this shows $\mathcal{I}_{\text{re}} \ll \mathcal{I}_{\text{im}}$ which justifies the approximation in Eqs. (3.15) and (3.16).

References

- [1] D. Baumann and L. McAllister, doi:10.1017/CBO9781316105733 arXiv:1404.2601 [hep-th].
- [2] M. Maggiore, Phys. Rept. **331**, 283 (2000) doi:10.1016/S0370-1573(99)00102-7 [gr-qc/9909001].

- [3] T. Matsumura *et al.*, J. Low. Temp. Phys. **176**, 733 (2014) doi:10.1007/s10909-013-0996-1 [arXiv:1311.2847 [astro-ph.IM]].
- [4] P. Amaro-Seoane *et al.*, Class. Quant. Grav. **29**, 124016 (2012) doi:10.1088/0264-9381/29/12/124016 [arXiv:1202.0839 [gr-qc]].
- [5] B. P. Abbott *et al.* [LIGO Scientific and Virgo Collaborations], Phys. Rev. Lett. **118**, no. 12, 121101 (2017) Erratum: [Phys. Rev. Lett. **119**, no. 2, 029901 (2017)] doi:10.1103/PhysRevLett.118.121101, 10.1103/PhysRevLett.119.029901 [arXiv:1612.02029 [gr-qc]].
- [6] N. Seto, S. Kawamura and T. Nakamura, Phys. Rev. Lett. **87**, 221103 (2001) doi:10.1103/PhysRevLett.87.221103 [astro-ph/0108011].
- [7] S. Kawamura *et al.*, Class. Quant. Grav. **28**, 094011 (2011). doi:10.1088/0264-9381/28/9/094011
- [8] M. C. Guzzetti, N. Bartolo, M. Liguori and S. Matarrese, Riv. Nuovo Cim. **39**, no. 9, 399 (2016) doi:10.1393/ncr/i2016-10127-1 [arXiv:1605.01615 [astro-ph.CO]].
- [9] N. Bartolo *et al.*, JCAP **1612**, no. 12, 026 (2016) doi:10.1088/1475-7516/2016/12/026 [arXiv:1610.06481 [astro-ph.CO]].
- [10] T. Namikawa, S. Saga, D. Yamauchi and A. Taruya, Phys. Rev. D **100** (2019) no.2, 021303 doi:10.1103/PhysRevD.100.021303 [arXiv:1904.02115 [astro-ph.CO]].
- [11] C. de Rham, Living Rev. Rel. **17**, 7 (2014) doi:10.12942/lrr-2014-7 [arXiv:1401.4173 [hep-th]].
- [12] S. Dubovsky, R. Flauger, A. Starobinsky and I. Tkachev, Phys. Rev. D **81**, 023523 (2010) doi:10.1103/PhysRevD.81.023523 [arXiv:0907.1658 [astro-ph.CO]].
- [13] A. E. Gumrukuoglu, S. Kuroyanagi, C. Lin, S. Mukohyama and N. Tanahashi, Class. Quant. Grav. **29**, 235026 (2012) doi:10.1088/0264-9381/29/23/235026 [arXiv:1208.5975 [hep-th]].
- [14] M. Fasiello and R. H. Ribeiro, JCAP **1507**, no. 07, 027 (2015) doi:10.1088/1475-7516/2015/07/027 [arXiv:1505.00404 [astro-ph.CO]].
- [15] S. Kuroyanagi, C. Lin, M. Sasaki and S. Tsujikawa, Phys. Rev. D **97**, no. 2, 023516 (2018) doi:10.1103/PhysRevD.97.023516 [arXiv:1710.06789 [gr-qc]].
- [16] T. Fujita, S. Kuroyanagi, S. Mizuno and S. Mukohyama, Phys. Lett. B **789**, 215 (2019) doi:10.1016/j.physletb.2018.12.025 [arXiv:1808.02381 [gr-qc]].
- [17] C. de Rham and G. Gabadadze, Phys. Rev. D **82**, 044020 (2010) doi:10.1103/PhysRevD.82.044020 [arXiv:1007.0443 [hep-th]].
- [18] C. de Rham, G. Gabadadze and A. J. Tolley, Phys. Rev. Lett. **106**, 231101 (2011) doi:10.1103/PhysRevLett.106.231101 [arXiv:1011.1232 [hep-th]].
- [19] A. Higuchi, Nucl. Phys. B **282**, 397 (1987). doi:10.1016/0550-3213(87)90691-2
- [20] A. De Felice and S. Mukohyama, Phys. Lett. B **752**, 302 (2016) doi:10.1016/j.physletb.2015.11.050 [arXiv:1506.01594 [hep-th]].
- [21] A. De Felice and S. Mukohyama, JCAP **1604**, no. 04, 028 (2016) doi:10.1088/1475-7516/2016/04/028 [arXiv:1512.04008 [hep-th]].
- [22] N. Arkani-Hamed, H. C. Cheng, M. A. Luty and S. Mukohyama, JHEP **0405**, 074 (2004) doi:10.1088/1126-6708/2004/05/074 [hep-th/0312099].
- [23] V. A. Rubakov, hep-th/0407104.
- [24] S. L. Dubovsky, JHEP **0410**, 076 (2004) doi:10.1088/1126-6708/2004/10/076 [hep-th/0409124].
- [25] D. Blas, D. Comelli, F. Nesti and L. Pilo, Phys. Rev. D **80**, 044025 (2009) doi:10.1103/PhysRevD.80.044025 [arXiv:0905.1699 [hep-th]].

- [26] D. Comelli, F. Nesti and L. Pilo, *JHEP* **1307**, 161 (2013) doi:10.1007/JHEP07(2013)161 [arXiv:1305.0236 [hep-th]].
- [27] D. Langlois, S. Mukohyama, R. Namba and A. Naruko, *Class. Quant. Grav.* **31**, 175003 (2014) doi:10.1088/0264-9381/31/17/175003 [arXiv:1405.0358 [hep-th]].
- [28] A. Ricciardone and G. Tasinato, *JCAP* **1802**, no. 02, 011 (2018) doi:10.1088/1475-7516/2018/02/011 [arXiv:1711.02635 [astro-ph.CO]].
- [29] A. Gruzinov, *Phys. Rev. D* **70**, 063518 (2004) doi:10.1103/PhysRevD.70.063518 [astro-ph/0404548].
- [30] S. Endlich, A. Nicolis and J. Wang, *JCAP* **1310**, 011 (2013) doi:10.1088/1475-7516/2013/10/011 [arXiv:1210.0569 [hep-th]].
- [31] A. Nicolis, R. Penco and R. A. Rosen, *Phys. Rev. D* **89**, no. 4, 045002 (2014) doi:10.1103/PhysRevD.89.045002 [arXiv:1307.0517 [hep-th]].
- [32] D. Cannone, G. Tasinato and D. Wands, *JCAP* **1501**, no. 01, 029 (2015) doi:10.1088/1475-7516/2015/01/029 [arXiv:1409.6568 [astro-ph.CO]].
- [33] N. Bartolo, D. Cannone, A. Ricciardone and G. Tasinato, *JCAP* **1603**, no. 03, 044 (2016) doi:10.1088/1475-7516/2016/03/044 [arXiv:1511.07414 [astro-ph.CO]].
- [34] A. Ricciardone and G. Tasinato, *Phys. Rev. D* **96**, no. 2, 023508 (2017) doi:10.1103/PhysRevD.96.023508 [arXiv:1611.04516 [astro-ph.CO]].
- [35] C. Cheung, P. Creminelli, A. L. Fitzpatrick, J. Kaplan and L. Senatore, *JHEP* **0803**, 014 (2008) doi:10.1088/1126-6708/2008/03/014 [arXiv:0709.0293 [hep-th]].
- [36] J. M. Maldacena, *JHEP* **0305**, 013 (2003) doi:10.1088/1126-6708/2003/05/013 [astro-ph/0210603].
- [37] J. M. Maldacena and G. L. Pimentel, *JHEP* **1109**, 045 (2011) doi:10.1007/JHEP09(2011)045 [arXiv:1104.2846 [hep-th]].
- [38] J. Soda, H. Kodama and M. Nozawa, *JHEP* **1108**, 067 (2011) doi:10.1007/JHEP08(2011)067 [arXiv:1106.3228 [hep-th]].
- [39] M. Shiraishi, D. Nitta and S. Yokoyama, *Prog. Theor. Phys.* **126**, 937 (2011) doi:10.1143/PTP.126.937 [arXiv:1108.0175 [astro-ph.CO]].
- [40] X. Gao, T. Kobayashi, M. Yamaguchi and J. Yokoyama, *Phys. Rev. Lett.* **107**, 211301 (2011) doi:10.1103/PhysRevLett.107.211301 [arXiv:1108.3513 [astro-ph.CO]].
- [41] Y. Huang, A. Wang, R. Yousefi and T. Zhu, *Phys. Rev. D* **88**, no. 2, 023523 (2013) doi:10.1103/PhysRevD.88.023523 [arXiv:1304.1556 [hep-th]].
- [42] T. Zhu, W. Zhao, Y. Huang, A. Wang and Q. Wu, *Phys. Rev. D* **88**, 063508 (2013) doi:10.1103/PhysRevD.88.063508 [arXiv:1305.0600 [hep-th]].
- [43] J. L. Cook and L. Sorbo, *JCAP* **1311**, 047 (2013) doi:10.1088/1475-7516/2013/11/047 [arXiv:1307.7077 [astro-ph.CO]].
- [44] M. Shiraishi, A. Ricciardone and S. Saga, *JCAP* **1311**, 051 (2013) doi:10.1088/1475-7516/2013/11/051 [arXiv:1308.6769 [astro-ph.CO]].
- [45] Y. Akita and T. Kobayashi, *Phys. Rev. D* **93**, no. 4, 043519 (2016) doi:10.1103/PhysRevD.93.043519 [arXiv:1512.01380 [hep-th]].
- [46] A. Agrawal, T. Fujita and E. Komatsu, *Phys. Rev. D* **97**, no. 10, 103526 (2018) doi:10.1103/PhysRevD.97.103526 [arXiv:1707.03023 [astro-ph.CO]].
- [47] A. Agrawal, T. Fujita and E. Komatsu, *JCAP* **1806**, no. 06, 027 (2018) doi:10.1088/1475-7516/2018/06/027 [arXiv:1802.09284 [astro-ph.CO]].

- [48] E. Dimastrogiovanni, M. Fasiello, G. Tasinato and D. Wands, JCAP **1902**, 008 (2019) doi:10.1088/1475-7516/2019/02/008 [arXiv:1810.08866 [astro-ph.CO]].
- [49] N. Bartolo *et al.*, JCAP **1811**, no. 11, 034 (2018) doi:10.1088/1475-7516/2018/11/034 [arXiv:1806.02819 [astro-ph.CO]].
- [50] N. Bartolo, V. De Luca, G. Franciolini, A. Lewis, M. Peloso and A. Riotto, Phys. Rev. Lett. **122**, no. 21, 211301 (2019) doi:10.1103/PhysRevLett.122.211301 [arXiv:1810.12218 [astro-ph.CO]].
- [51] N. Bartolo, V. De Luca, G. Franciolini, M. Peloso, D. Racco and A. Riotto, Phys. Rev. D **99**, no. 10, 103521 (2019) doi:10.1103/PhysRevD.99.103521 [arXiv:1810.12224 [astro-ph.CO]].
- [52] D. Jeong and M. Kamionkowski, Phys. Rev. Lett. **108** (2012) 251301 doi:10.1103/PhysRevLett.108.251301 [arXiv:1203.0302 [astro-ph.CO]].
- [53] L. Dai, D. Jeong and M. Kamionkowski, Phys. Rev. D **88** (2013) no.4, 043507 doi:10.1103/PhysRevD.88.043507 [arXiv:1306.3985 [astro-ph.CO]].
- [54] S. Brahma, E. Nelson and S. Shandera, Phys. Rev. D **89** (2014) no.2, 023507 doi:10.1103/PhysRevD.89.023507 [arXiv:1310.0471 [astro-ph.CO]].
- [55] E. Dimastrogiovanni, M. Fasiello, D. Jeong and M. Kamionkowski, JCAP **1412** (2014) 050 doi:10.1088/1475-7516/2014/12/050 [arXiv:1407.8204 [astro-ph.CO]].
- [56] G. Janssen *et al.*, PoS AASKA **14**, 037 (2015) doi:10.22323/1.215.0037 [arXiv:1501.00127 [astro-ph.IM]].
- [57] M. Tsuneto, A. Ito, T. Noumi and J. Soda, JCAP **1903**, no. 03, 032 (2019) doi:10.1088/1475-7516/2019/03/032 [arXiv:1812.10615 [gr-qc]].
- [58] S. Weinberg, Phys. Rev. D **72**, 043514 (2005) doi:10.1103/PhysRevD.72.043514 [hep-th/0506236].
- [59] M. S. Turner, M. J. White and J. E. Lidsey, Phys. Rev. D **48**, 4613 (1993) doi:10.1103/PhysRevD.48.4613 [astro-ph/9306029].
- [60] E. Dimastrogiovanni, M. Fasiello and G. Tasinato, JCAP **1808**, no. 08, 016 (2018) doi:10.1088/1475-7516/2018/08/016 [arXiv:1806.00850 [astro-ph.CO]].
- [61] O. Ozsoy, M. Mylova, S. Parameswaran, C. Powell, G. Tasinato and I. Zavala, arXiv:1902.04976 [hep-th].
- [62] E. Pajer, F. Schmidt and M. Zaldarriaga, Phys. Rev. D **88**, no. 8, 083502 (2013) doi:10.1103/PhysRevD.88.083502 [arXiv:1305.0824 [astro-ph.CO]].
- [63] L. Bordin, P. Creminelli, M. Mirbabayi and J. Norea, JCAP **1609**, no. 09, 041 (2016) doi:10.1088/1475-7516/2016/09/041 [arXiv:1605.08424 [astro-ph.CO]].
- [64] S. Endlich, B. Horn, A. Nicolis and J. Wang, Phys. Rev. D **90**, no. 6, 063506 (2014) doi:10.1103/PhysRevD.90.063506 [arXiv:1307.8114 [hep-th]].
- [65] M. Akhshik, JCAP **1505**, no. 05, 043 (2015) doi:10.1088/1475-7516/2015/05/043 [arXiv:1409.3004 [astro-ph.CO]].
- [66] L. Bordin, P. Creminelli, M. Mirbabayi and J. Norea, JCAP **1703**, no. 03, 004 (2017) doi:10.1088/1475-7516/2017/03/004 [arXiv:1701.04382 [astro-ph.CO]].
- [67] E. Pajer, S. Jazayeri and D. van der Woude, JCAP **1906**, no. 06, 011 (2019) doi:10.1088/1475-7516/2019/06/011 [arXiv:1902.09020 [hep-th]].
- [68] N. Arkani-Hamed and J. Maldacena, arXiv:1503.08043 [hep-th].
- [69] H. Lee, D. Baumann and G. L. Pimentel, JHEP **1612**, 040 (2016) doi:10.1007/JHEP12(2016)040 [arXiv:1607.03735 [hep-th]].

- [70] A. Kehagias and A. Riotto, *JCAP* **1707** (2017) no.07, 046 doi:10.1088/1475-7516/2017/07/046 [arXiv:1705.05834 [hep-th]].
- [71] M. Biagetti, E. Dimastrogiovanni and M. Fasiello, *JCAP* **1710**, no. 10, 038 (2017) doi:10.1088/1475-7516/2017/10/038 [arXiv:1708.01587 [astro-ph.CO]].
- [72] G. Franciolini, A. Kehagias and A. Riotto, *JCAP* **1802** (2018) no.02, 023 doi:10.1088/1475-7516/2018/02/023 [arXiv:1712.06626 [hep-th]].
- [73] G. Franciolini, A. Kehagias, A. Riotto and M. Shiraishi, *Phys. Rev. D* **98** (2018) no.4, 043533 doi:10.1103/PhysRevD.98.043533 [arXiv:1803.03814 [astro-ph.CO]].
- [74] L. Bordin, P. Creminelli, A. Khmelnitsky and L. Senatore, *JCAP* **1810** (2018) no.10, 013 doi:10.1088/1475-7516/2018/10/013 [arXiv:1806.10587 [hep-th]].
- [75] G. Goon, K. Hinterbichler, A. Joyce and M. Trodden, arXiv:1812.07571 [hep-th].
- [76] D. Anninos, V. De Luca, G. Franciolini, A. Kehagias and A. Riotto, *JCAP* **1904**, no. 04, 045 (2019) doi:10.1088/1475-7516/2019/04/045 [arXiv:1902.01251 [hep-th]].
- [77] L. Bordin and G. Cabass, *JCAP* **1906** (2019) no.06, 050 doi:10.1088/1475-7516/2019/06/050 [arXiv:1902.09519 [astro-ph.CO]].
- [78] E. Dimastrogiovanni, M. Fasiello and G. Tasinato, arXiv:1906.07204 [astro-ph.CO].
- [79] M. Shiraishi, *Front. Astron. Space Sci.* **6** (2019) 49 doi:10.3389/fspas.2019.00049 [arXiv:1905.12485 [astro-ph.CO]].